Bar-Ilan University

Observation of Coherent Oscillations in Molecular Association from Ultra Cold Thermal Gas

Roy Elbaz

Submitted in Partial Fulfillment of the Requirements for the
Master's Degree in the Department of Physics,
Bar-Ilan University

Ramat-Gan, Israel 2021

This Work Was Carried Out Under The Supervision Of Prof. Lev Khaykovich of the Department of Physics, Bar-Ilan University.

Contents

List of Figures

List of Tables

Abstract

Today it is common knowledge that a two level system can exhibit the famous Rabi oscillations when a resonant pulse, which couples the 2 levels, is applied. Since the discovery of this phenomena, there has been much advancement in this direction. Starting from the Ramsey sequence, which utilize the subtle control of the Rabi pulse over the population of each level, and onto much more complicated processes, often elegantly described by the Bloch sphere.

By replacing one of the two levels with an energy continuum, a more complicated scheme must be considered, and Rabi oscillations are rather unattainable. This kind of system can be found in ionization processes in which a bound electron state is coupled to free electron continuum. Another scenario, and more relevant to this story, is the case of molecule formation out of individual free atoms. The latter contain a vastly growing subdomain called Feshbach molecules.

Due to the ultra low temperatures achieved in a cold atoms apparatus these days, it is possible to rather easily utilize the advantages of Feshbach theory of collisional resonances. It predicts the existence of inter-channels resonances which allows us to form weakly bound molecules out of free atoms. The highlight of this phenomena is that we can tweak the binding energy using an external magnetic field.

In this work, we will describe a phenomena in which an oscillatory drive is applied on a continuum + bound level system, and oscillations in the population do appear, however it is different by nature from the famous Rabi oscillations. The phenomena is called Stückelberg oscillations, and it is a non-adiabatic effect, related to the pulse envelop, so far only observed in ionization processes by ultra short pulses [1]. The theory for this process has been suggested in [2], and we set to our selves to realize it on out ultra

cold atoms system. The experimental results shown here shed light on the behavior of such systems under an oscillatory drive, and are crucial for better understanding of many similar processes.

1 Introduction

Oscillatory drive to a quantum system is one of the most frequently used procedures. It has a role in uncountable number of fields, such as atomic and molecular physics [3–8], quantum computing [9, 10], ultra-fast processes [1, 11], and many others. Although quantum physics has been around for more than a century, and oscillatory drive for longer than that, the properties of such an interaction are still being investigated and there is still much to learn.

With the ability to cool atoms into the quantum degeneracy regime, where the De-Broglie wavelength becomes of the order of the inter-particle distance, came the opportunity for exploring the behavior of systems that were previously unaccessible [12]. This has opened the gate for a veriety of experiments, some of them on the well known two-level system.

This breakthrough has also led to great advancement in the field of atomic and molecular physics. It can be shown [13] that the interaction between two particles in the limit of ultra-cold temperatures can be universally described by a single parameter, the scattering length. The scattering length can be intuitively understood as a measure of the interaction strength between the two particles. The truly remarkable effect is that in some conditions, the scattering length can diverge. This is referred to as a "Feshbach resonance". This is caused due to coupling between 2 different spin channels, and it can usually be tuned using an external magnetic field. In the area of positive scattering length a weakly bound molecular state exists, called a "Feshbach molecule". One vastly used technique of producing such molecules is by applying a magnetic modulation at RF frequencies. This was first demonstrated in [3]. In this paper, Rabi like oscillations were presented for the population of the molecular state as a function of the pulse duration.

However, more recent theoretical treatments [2, 14] have shown that under the parameters Wieman et al. have been using, such Rabi like oscillations should not appear. This thesis brings new data that sheds light on this many years conundrum. We will also give first experimental evidence to a new type of a coherent process in the field of molecule production out of ultra cold thermal gas, as suggested in [2].

2 Theoretical background

2.1 Two-level system

In order to get a better understanding of the phenomena described in this work, we must first start with a simple model. That is the quantum system that has 2 energy states, and up to a certain approximation, it is decoupled from any other state. Thus we can describe a general wave function as a superposition of those 2 states

$$|\psi\rangle = c_g |g\rangle + c_e |e\rangle$$

We'll set the ground state energy to be zero, and so the Hamiltonian of the system is

$$\hat{\mathcal{H}}_{bare} = \begin{pmatrix} 0 & 0 \\ 0 & \hbar\omega_0 \end{pmatrix}$$

where $\hbar\omega_0$ is the energy difference between the two levels. We consider an oscillatory drive which couples the 2 levels such that the total Hamiltonian is $\hat{\mathcal{H}}_{tot} = \hat{\mathcal{H}}_{bare} + \hat{\mathcal{H}}_{osc}$, where

$$\hat{\mathcal{H}}_{osc} = \begin{pmatrix} 0 & d_{eg} \\ d_{eg} & 0 \end{pmatrix} cos(\omega_L t)$$

and $d_{eg}cos(\omega_L t)$ is the matrix element for the coupling Hamiltonian, and ω_L is the angular frequency of the oscillatory coupling.

By solving the Schrödinger equation, under the initial condition of $c_g(t = 0) = 1$, we get the probability of finding a system in the excited state:

$$|c_e(t)|^2 = \left(\frac{\Omega}{\Omega_R}\right)^2 sin^2(\frac{\Omega_R t}{2})$$

where $\Omega = \frac{d_{eg}}{\hbar}$ is the famous Rabi frequency, $\Omega_R = \sqrt{|\Omega|^2 + \delta^2}$ is known as the generalized Rabi frequency, and $\delta = \omega_L - \omega_0$ is the frequency detuning of the driving field relative to the energy difference.

In this solution we can see that the system oscillates between the ground state and the excited state at a frequency $\frac{\Omega_R}{2\pi}$. Another important term is a "π pulse", in which a particle undergoes half a Rabi-cycle (thus the name), and so if that particle began in the ground state, it will move with absolute certainty to the excited state. However, this is true only if the driving field frequency matches exactly to the transition frequency (i.e $\delta = 0$). In case of non-zero detuning, the probability of being in the excited state after half a cycle is

$$P_e = \frac{1}{1+\left(\frac{\delta}{\Omega_R}\right)^2} sin^2\left(\frac{\tau}{2}\sqrt{\Omega_R^2 + \delta^2}\right)$$

The probability will be at its maximum when $\tau = \frac{\pi}{\sqrt{\Omega_R^2+\delta^2}}$, and as a function of the detuning, the maximal probability will have a Sinc square shape with a FWHM of $2\Omega_R$.

Rabi first used this technique for measuring particle transition frequencies. It can be seen that in order to pin down the frequency more precisely, it is in our best interest to decrease Ω_R. However, the constraint of $\Omega_R \sim \frac{\pi}{\tau}$ when $\delta \to 0$ dictates that we should increase τ, the time that the particle spends in the interaction zone. Experimental complexities which stems from this requirement ultimately limit the level of precision that can be achieved.

As a way of tackling this obstacle, Rabi's student, Norman Ramsey came with a different approach, which utilizes Rabi's theory, and brings greater precision by introducing two separate interaction zones.

What Ramsey suggested was applying two "$\pi/2$ pulse" with a time gap T between

them. Similarly to the "π pulse", the "$\pi/2$ pulse" is when the atom undergoes a quarter of a Rabi cycle during the time in which the field is on. It therefore goes into a superposition of both the ground and the excited state. It then accumulates a phase for each state according to the bare Hamiltonian $e^{-i\frac{E_g+\hbar\omega_L}{\hbar}t}$ and $e^{-i\frac{E_{g/e}}{\hbar}t}$, after which the second "$\pi/2$ pulse" interferes the two states and we get again oscillations in the excited state population due to the different evolution pace of each state. [15].

In this approach, the probability of finding an atom in the excited state for small detuning (i.e $\delta \ll \Omega_R$) is

$$P_e = cos^2\left(\frac{\delta T}{2}\right)$$

and the precision now goes like the time T, but here, it is the time between the pulses, in which the interaction is off. Experimentally, this is much easier to control, and greater precision can be obtained.

This is essentially a new kind of an interferometer, in which the 2 pathways are the 2 quantum states of the atom, and the bare energy time evolution during the gap between the pulses is where the phase accumulation occurs. Each "$\pi/2$ pulse" acts as a beam splitter for the wave function.

Another way of looking at this system is in the *dressed* basis. This is the eigen basis of the Hamiltonian. Once solving in that basis, one can see that there is a shift in energies $\Delta E = \frac{1}{2}\frac{|\Omega_R|^2}{\delta}$ which is also referred to as the AC-Stark shift. As we shall see, this plays a crucial part in our phenomena.

All that is described above mostly apply for the ideal case of a two level system. In any experimental apparatus, there are non-ideal effects that must be taken into account. Rabi and Ramsey sequences are usually performed on an ensemble of atoms, what leads to broadnings and decoherence mechanisms. Most of them relate to the fact that different

atoms have different Rabi frequencies. This can be caused by velocities distribution, the width of the 2 levels and more.

Since the discovery of the Rabi and Ramsey sequences, there have been innumerous of experiments and theories which carried their names due to the unique characteristics in each of them.

2.2 Discrete level coupled to a continuum

The previous section describes the case of a system with 2 discrete energy levels (and nothing more) containing a single particle. This is of course an approximation of any system we can find in the world around us. Even if we take a system and look at a subspace of 2 energy levels, ignoring all the others, still no experimental apparatus can generate a system of 2 truly discrete energy levels. On top of all the technical difficulties, there will always be some probability of spontaneous decay from the excited state into the ground state. This introduce a finite width to the energy levels which cause the damping of the oscillations to the steady state solution.

In addition, these experiments are usually performed on an ensemble of atoms, which leads to broadenings and decoherence mechanisms. For example, different atoms have different velocities, causing the known Doppler broadening. Collisions between the atoms add random phase shifts to their wave function. These effects and others cause decoherence of the system and the decay of oscillations.

The finite width and the ensemble effects generate a distribution of Rabi frequencies. Thus any observable, such as the excited state population, must be averaged over this distribution. This may have destructive influence on the ability to observe the Rabi cycle, but when examined, the parameters must be taken with relative perspective. As in every

damped oscillator, as long as the damping typical time scale is larger than the time period of the oscillations, they can still be observed.

Here, the damping typical time scale goes as $\sim \frac{1}{\sigma_E}$ where σ_E represent the energy width caused by the inherent level width and the energy distribution of atoms due to broadenings. With ultra cold atoms, and the inner-atomic states acting as the effective two level system, the damping time scale can be rather easily made long enough for observing many oscillations.

In this work we will discuss a similar case in which there is one (nearly) discrete level, and an energy continuum distanced from that level. The story here becomes more complicated since we must take into account the coupling of all the possible states within the continuum with the discrete level. We will focus on the widely investigated system of molecule formation out of ultra cold atom gas. The molecular state is a discrete bound state (in the center of mass motion frame) by nature since the 2 atoms are bound to one another. And the two-body continuum is an ensemble of free atoms, with a Maxwell-Boltzmann distribution of the relative motion. The width of the continuum is $\sim k_B T$, where k_B is the Boltzmann constant and T is the temperature of the system.

In this scenario, the typical width of the continuum found in experimental systems to date is too large and overdamping demolishes the chance of observing Rabi oscillations. Of course once Rabi sequence is unattainable, there's no point of talking about Ramsey sequence. The phenomena described in this thesis unravel a different oscillatory behavior, driven by a different mechanism, and of great importance to the field of molecular and atomic physics.

2.3 Feshbach molecules

When analyzing the scenario of two atoms collision, it is convenient to work in the center of mass coordinate system with the center of mass location $R_{CM} = \frac{m_1\vec{r_1}+m_2\vec{r_2}}{m_1+m_2}$ and the relative distance $\vec{r} = \vec{r_1} - \vec{r_2}$. Due to the interaction between the atoms, there is a potential energy which varies as a function of $\vec{r}$, and can possess molecular bound states. Since generally the interaction depends on the specific spin state in which the atoms enter the collision, there are different potential energy curves for each of those states as can be seen in Fig. 1. The potential energy curve that corresponds to the initial spin state of the two free atoms is referred to as the open channel, and the one for some other spin state is the closed channel. There can be various scenarios for different systems, but they can all be described that way. With that in mind, it is clear that the background potential energy for free atoms, and the bound states' energy levels are generally different from one potential curve to another, depending on their joint spin state. Consider two atoms approaching each other (starting from $\vec{r} \to \infty$) with a certain spin state (the open channel) and a total entrance energy E_{in}. Now, if another spin state is coupled to the open channel, and has a bound energy level with energy E_c that is equal to E_{in} then the coupling becomes resonant, and the atoms can change their spin state, jump to the resonant bound level, and form a Feshbach molecule.

The highlight of this domain is the following: if one (or both) of the potentials has a non zero (non equal) total spin, it (they) can often be tuned by an external magnetic field due to the Zeeman effect. This allows the adjustment of energy levels, both bound and continuum. This is a remarkable method that allows us to achieve a Feshbach resonance more easily, as they are somewhat rare to be found in natural systems. For example, we can tune the closed channel curve until one of the bound energy levels coincides with the

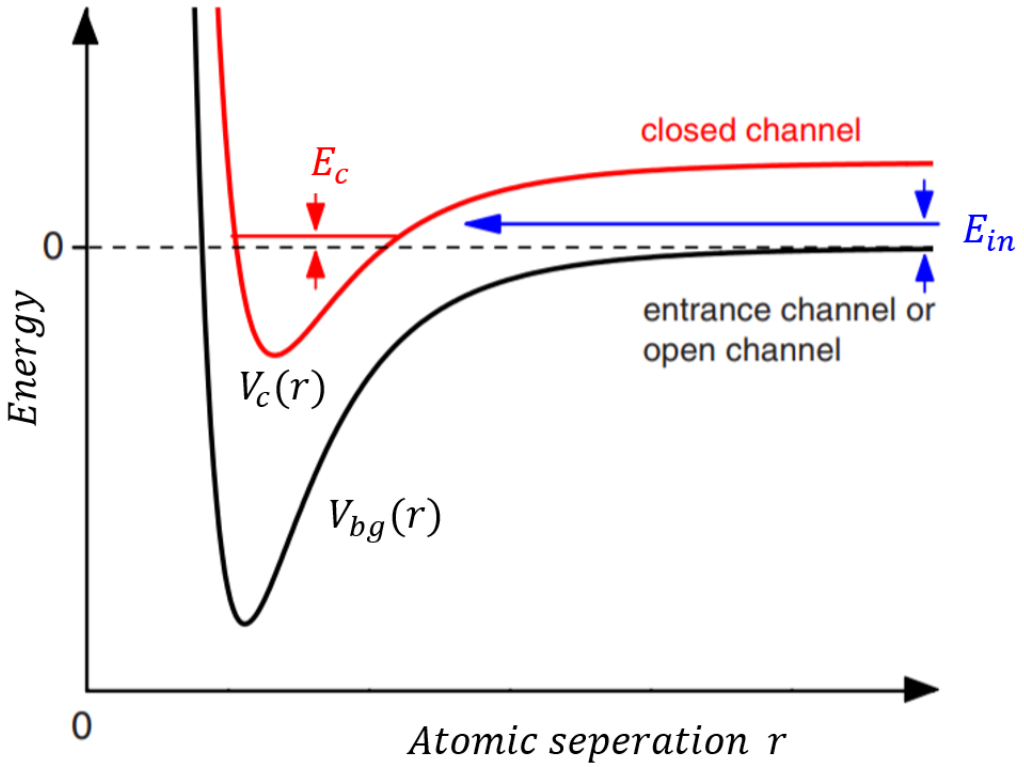

Fig. 1. Energy scheme for the 2 atoms' system (Fig. 1 in ref. [13]). The black curve $V_{bg}(R_r)$ is the potential energy as a function of the distance between the atoms, for 2 free atoms in some initial joint spin state. They approach each other with a total energy E_{in}. The red curve is the potential energy $V_c(R_r)$ for the closed channel that corresponds to a different spin state. A resonance will occur when one of the bound energy levels E_c resonantly couples to the entrance energy E_{in}.

free atoms entrance energy E_{in}. It is also possible to tune the bound levels' energies such that there will be an energy difference between E_c and E_{in}. The transition can then be stimulated by an external electromagnetic pulse at the correct frequency.

As in every 2-body system, the angular momentum part of the effective potential energy is repulsive and becomes larger as l increases. So it can be shown that for ultra-cold bosons, with $k \to 0$, the collision is mostly determined by S-wave ($l = 0$) scattering and can be described by a single parameter, the scattering length a. a is essentially a

measure for the interaction strength between the atoms, with positive scattering length meaning attractive interaction and negative meaning repulsive. When the bound level resonantly couples to the entrance level, the scattering length diverges. It can be shown [13] that the binding energy of 2 atoms close to the resonance can be approximated as a function of the scattering length $E_b = -\frac{\hbar^2}{ma^2}$. It can be easily understood that varying one of the potentials (e.g by changing the magnetic field) affects the interaction between 2 atoms, and therefore affects the scattering length. In this case the dependence of a in the magnetic field is $a(B) = a_{bg}(1 - \frac{\Delta}{B-B_0})$ with a_{bg} being the background scattering length at $B \to \infty$ (i.e far from resonance), B_0 the resonance magnetic field, and Δ is the resonance width [13]. Therefore, as described before, by changing the DC magnetic field, one can tune the binding energy. This is illustrated in Fig. 2.

2.4 Threshold in Feshbach molecule association

Besides being the heart of a whole new sub-domain in physics, Feshbach theory introduces a remarkable molecule production method that enables us to isolate various quantum effects with unprecedented control. Feshbach molecules are also interesting since they are weakly bound creatures with a much larger spatial extent than the free atoms they were created from. There are several experimentally demonstrated methods of producing Feshbach molecules. The 2 most common methods are Feshbach ramps and oscillatory fields [13].

Feshbach ramps method involves sweeping the magnetic field across the Feshbach resonance. The resonant interaction crossed during this procedure produces molecules with relatively high efficiency, in some cases up to 80% [16]. This method has the disadvantage of unwanted heating effect. In ref. [3] they report of ^{85}Rb heated by a factor of 250 (a

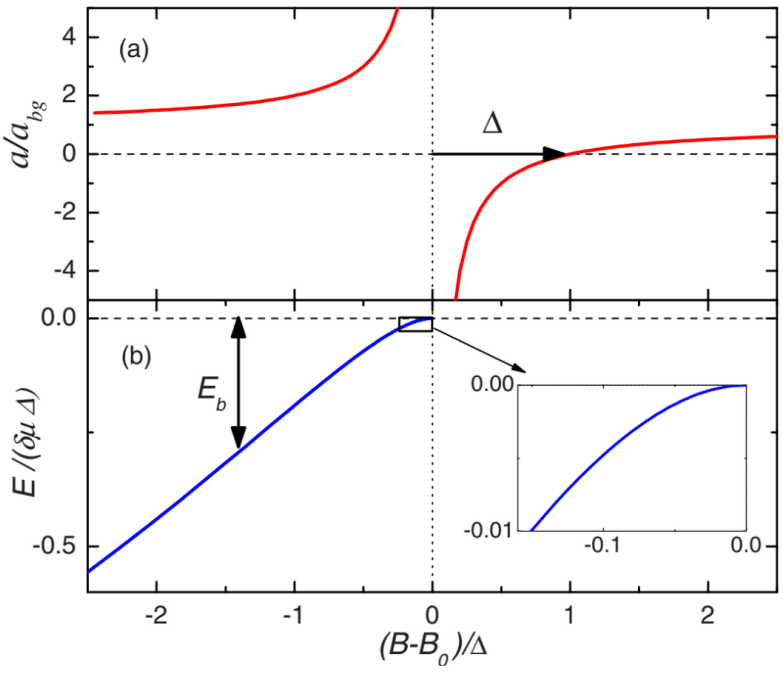

Fig. 2. Properties of a Feshbach resonance (Fig. 2 in ref. [13]). (a) Scattering length as a function of the external magnetic field. A clear resonance can be seen where the scattering length diverges. (b) Feshbach molecule energy as a function of the magnetic field. The molecule exists where the scattering length is positive. At the resonance the energy coincide with the continuum.

few μK) during the field sweep.

The relevant method for our experiment is the second one, in which the magnetic field is set such that there is a weakly bound molecular level with energy $-E_b$, with $E = 0$ the zero kinetic energy of the thermal gas. Next, a modulation of the magnetic field is applied such that

$$B(t) = B_{dc} + b\ sin(\omega t)$$

Since the magnetic field couples the 2 channels of the 2-atoms system, the modulation can stimulate molecule production. This method has been first demonstrated experimentally in [3], and breached the way to a new method of producing Feshbach molecules while

avoiding a few limiting properties of the Feshbach ramps method. The production of molecules is optimal when the modulation frequency ω is in proximity to the energy difference between the molecular level and the maximal population of the free atoms according to the Maxwell-Boltzmann distribution, i.e when $\hbar\omega \approx E_b$. The exact value is still being investigated by us together with a group of theoreticians, but we know that it is around that value up to a shift of $\sim k_B T$.

In ref. [3] one interesting figure shows the behavior of the molecular conversion efficiency (P_{MCE} of just MCE) as a function of the pulse duration. This is essentially the same feature discussed in sections 3.1 and 3.2. In this paper they present an oscillatory behavior with a frequency that is very close to the binding energy of their system. A theoretical paper published 2 years later claims that in the range of parameters used by Wieman et al. oscillations are smeared out due to decoherence. This, together with the similarity between the oscillations' frequency and the binding energy, caused the results shown in [3] to remain ambiguous to this day. In the next section we will review a new theoretical treatment which sheds light on the behavior of such a system, and will be the theory we set to ourselves to validate.

2.5 Coherence in Feshbach molecule association

Now we get to the heart of this thesis. As described in section 3.1 and 3.2, any finite width of each of the 2 levels will cause decoherence effects. In the case of molecule production out of ultra cold thermal gas, the width of the continuum is usually too large so coherency is significantly lost and oscillations cannot be observed. In this section we will dive into the details of this system and describe why Rabi sequence fails. Moreover, we will show a different protocol, called Stückelberg oscillations, which can bring coherence back into

the system. The model we will describe here was suggested in a theoretical paper [2].

For the treatment of this scenario we will consider a Hamiltonian $H = H_0 + \eta(r,t)cos(\omega t)$ where $\eta(r,t) = \eta_0\Theta(r_0 - r)\chi(t)$, $\omega/2\pi$ is the modulation frequency and $\chi(t)$ is the modulation time dependent amplitude (pulse envelope), and $\Theta(r)$ is a step function. The unperturbed Hamiltonian H_0 has one molecular bound level $|\phi_b\rangle$ and thermal states $|\epsilon\rangle$ with a Maxwell-Boltzmann distribution. Our general wave function is $|\psi\rangle = \sum_\alpha C_\alpha(t)e^{-i\frac{E_\alpha}{\hbar}t}|\alpha\rangle$, where $|\alpha\rangle$ are the eigenstates of H_0 . Plugging this into to the time dependent Schrödinger equation gives the set of equations for the coefficients:

$$i\hbar\partial_t C_b(t) = \Gamma_{bb}(t)C_b(t) + \int d\epsilon \Gamma_{b\epsilon}(t)e^{i\frac{E_b-\epsilon}{\hbar}t}C_\epsilon(t)$$

$$i\hbar\partial_t C_\epsilon(t) = \Gamma_{\epsilon b}(t)e^{-i\frac{E_b-\epsilon}{\hbar}t}C_b(t) + \int d\epsilon' \Gamma_{\epsilon\epsilon'}(t)e^{i\frac{\epsilon-\epsilon'}{\hbar}t}C_{\epsilon'}(t)$$

Where $\Gamma_{\alpha\beta} = cos(\omega t)\langle\alpha|\eta(r,t)|\beta\rangle$. These equations are solved numerically in Ref. [2] for ^{85}Rb atoms and then averaged over Maxwell Boltzmann distribution for the initial ensemble of states $|\epsilon\rangle$. We are interested in the MCE, which is the percentage of molecules produced out of the free atoms in the trap prior to applying the pulse, i.e $P_{MCE} = \frac{2N_m}{N_0} = \frac{N_0 - N_f}{N_0}$, where N_0 is the number of atoms prior to the pulse, N_f the number of atoms after the pulse, and N_m the number of molecules after the pulse. As can be seen in Fig. 3, for large modulation amplitude ($\eta_0/\hbar$), oscillations in the MCE can be observed, whereas for small amplitude, the system exhibits a monotonic increase of MCE as a function of the modulation duration. The threshold amplitude needed for observing significant oscillations is $\eta_C \approx 2\sqrt{-\frac{E_b+\hbar\omega}{\Delta}}$, where $\Delta = \mathcal{P}\int d\epsilon \frac{|W_{b\epsilon}|^2}{\epsilon - E_b - \hbar\omega}$, $\mathcal{P}\int$ stands for the principle integral and $W_{b\epsilon} = \Gamma_{b\epsilon}/(\eta_0 cos(\omega t))$.

To understand more intuitively the condition for observing oscillations, we can think of the diagram presented in Fig. 4. Free atoms obey Maxwell Boltzmann distribution

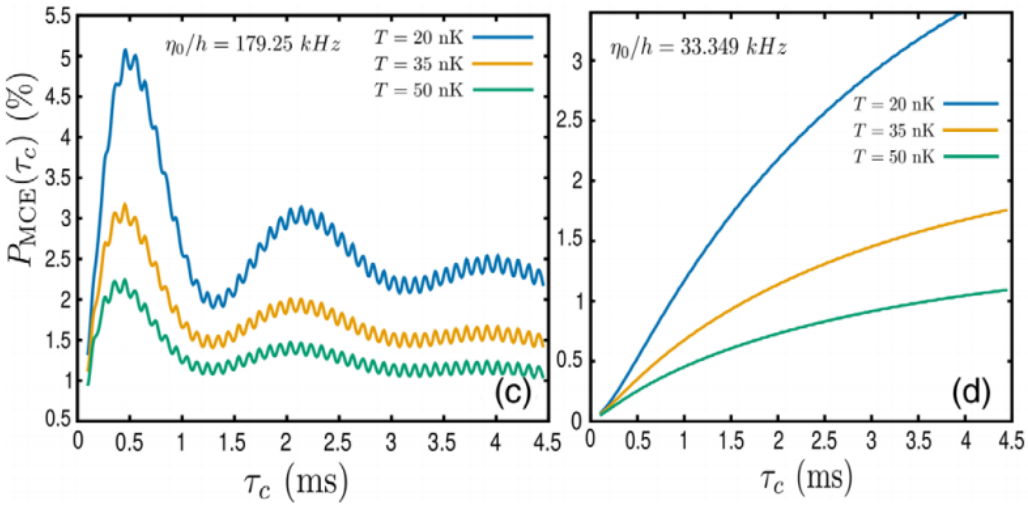

Fig. 3. MCE as a function of pulse plateau duration as presented in Fig. 1 in ref. [2].

and are represented by the shaded area. The dashed blue line marks a single energy level out of the free atoms continuum, and the red line is the molecular state in the dressed basis, so its energy in the beginning of the pulse becomes $-E_b + \hbar\omega$, with $\frac{\omega}{2\pi}$ being the RF modulation frequency, chosen to be slightly higher than the dissociation frequency. The oscillatory drive causes an AC Stark shift, so the bound level is shifted downwards by a magnitude proportional to the modulation amplitude squared (this relation will be derived in section 4.2.4). In this diagram one can see the pulse's envelope $\chi(t)$ in the form of the molecular state shift.

Now we get to the most important feature of this process. In order for this protocol to work, it must be non adiabatic, i.e the rise and fall time of the pulse need to be shorter compared to the typical timescale of the system, which in this case is $\frac{h}{k_B T}$. This non-adiabatic change of the Hamiltonian causes the initial wave packet, composed of the thermal distribution, to project itself onto the new Hamiltonian eigen states, and so a pair of free atoms form a superposition of the free state and the molecular state as the pulse is

turned on. Once the amplitude gets to its maximal value it remains there for a duration τ. During this stage the superposition accumulate phase in the 2 different channels (dashed red and green). As the pulse is turned off, that superposition is projected back onto the decoupled free and molecular states. This is essentially an interferometer in which the beginning and end of the pulse act as the beam-splitter.

Due to the Maxwell-Boltzmann distribution of the thermal gas, the interference for all the initial atom-pair states $|\epsilon\rangle$ must be accounted for, and different oscillation frequencies are averaged out. So this brings clarity to the condition of the threshold amplitude. In order to observe significant oscillations in the MCE, the thermal states' energy must be far from the molecular channel compared to the width of the continuum $k_B T$. We can think of a case in which the shift takes the molecular level somewhere inside the continuum. In that case, there are thermal states above and beneath the bound state, so they can have opposite phase and effectively cancel each other's oscillations.

If we examine the adiabatic limit of this process, we know that a pair of atoms, originating from the thermal gas, will always stay in the ground state. So as the pulse is turned on, and the coupling appears, the atoms will go into the molecular level as it traverse their initial kinetic energy. They will stay in that state until the turn off of the pulse, where they will dissociate back into free atoms. Basically, since the efficiency of this molecule production method depends on other parameters, such as the density, some atoms may not go into the molecular state, but the important thing to notice is that no superposition is created in this process, and there will not be any chance of oscillations.

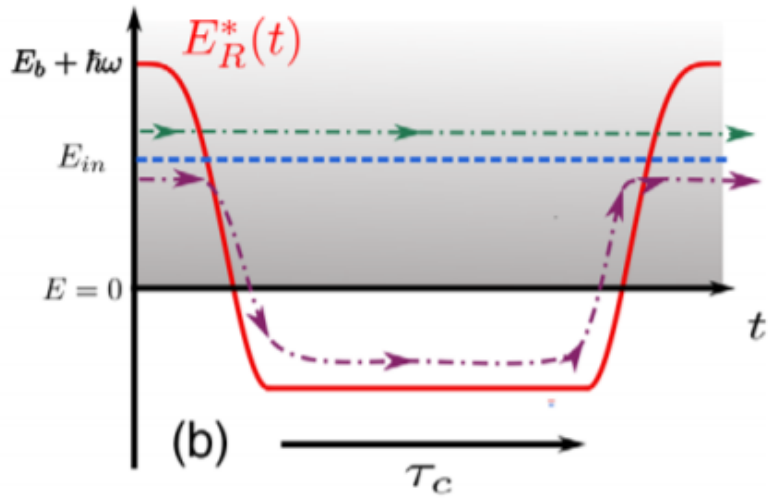

Fig. 4. Energy scheme during the RF pulse. The shaded area denotes the thermal distribution of the free atom and the red line represents the bound level energy plus the $\hbar\omega$. The dashed green and purple lines represent the two pathways the atoms can take. If the energy shift for the bound state exceeds the thermal distribution width, interference can be observed (Fig. 1 in ref. [2]).

3 Experiment

3.1 Experimental apparatus

3.1.1 Ultra cold atoms system

For successfully conducting this experiment we must have atoms at low temperatures. Therefore it is optimal to work with an ultra-cold atoms system. A brief description of it is given here along with a schematic diagram of the system in Fig. 5. Detailed explanation can be found in Ref [17]. Our cooling process is composed out of several steps. ^7Li atoms travel in a collimated beam towards a glass chamber through a Zeeman slower. We then use magneto-optical trap to catch the atoms in a $\sim 3mm$ cloud at a temperature of $\sim 1mK$. Next we use a $1064nm$ YAG laser to form a crossed beam dipole trap, in which we catch $\sim 3 \cdot 10^4$ atoms at a temperature of $\sim 1\mu K$. This temperature is achieved using evaporive cooling, during that stage the bias magnetic field is changed in several steps to $\sim 880Gauss$ (during which it crosses a Feshbach resonance at $845G$). In this field the binding energy is of the order of a few MHz.

3.1.2 RF pulse generator

The key process of our experiment is the production of molecules. We perform this by applying a magnetic field modulation at the frequency equal to the binding energy of the Feshbach molecules. Of course this quantity depends on the initial kinetic energy of a pair of atoms, and so it obeys the same distribution. We apply this modulation by a coil which creates a magnetic field in the same direction as the existing magnetic field bias [See Fig. 6].

As shown in section 3.5, a crucial condition for observing oscillations is to apply this

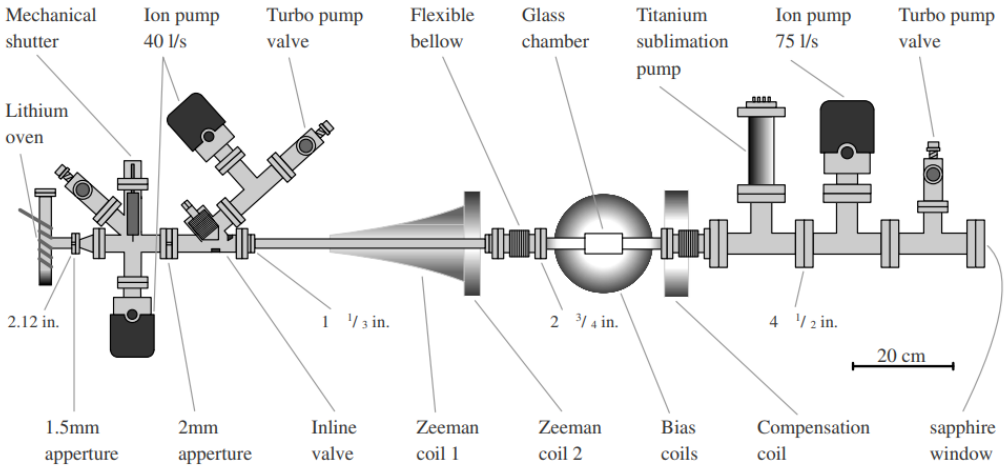

Fig. 5. Cold atoms system layout (Fig 1.1 in ref. [17]).

modulation with a high enough amplitude. The association frequency in our experiment is in the RF regime (i.e the order of a few MHz), for which the coil's impedance $Z_L = i\omega L$ prevents high amplitude currents from running through it. In order to solve this problem, we have connected a capacitor in series to the coil. This leads to the coil being the inductor of an LC circuit. Since the capacitor impedance is $Z_C = \frac{1}{i\omega C}$ there is a resonance frequency $f_r = \frac{\omega_r}{2\pi} = \frac{1}{2\pi\sqrt{LC}}$ in which the impedance of the coil and the capacitor cancel out and the maximum current amplitude $I_{max} = \frac{V_0}{R}$ is achieved, where V_0 is the voltage amplitude provided by the power supplier and R is the total DC resistance of the circuit. Since we need a high current to pass through our circuit, a normal voltage amplifier would not suffice. Instead, we use a MOSFET switching circuit to provide the alternating current to the antenna. In Fig. 6 it is possible to see a schematic drawing of that circuit with an IXRFD630 RF MOSFET driver in the heart of it. A power supplier is connected to the driver providing a constant voltage of 15V. An arbitrary function generator provides a square signal which alternately opens the MOSFET's gate at the desired frequency. The output of the driver is connected to the LC circuit which filters out only the resonance

frequency, to which we set the square signal's frequency in order to obtain maximal current. We therefore get a high amplitude sine wave signal at the antenna with the desired frequency.

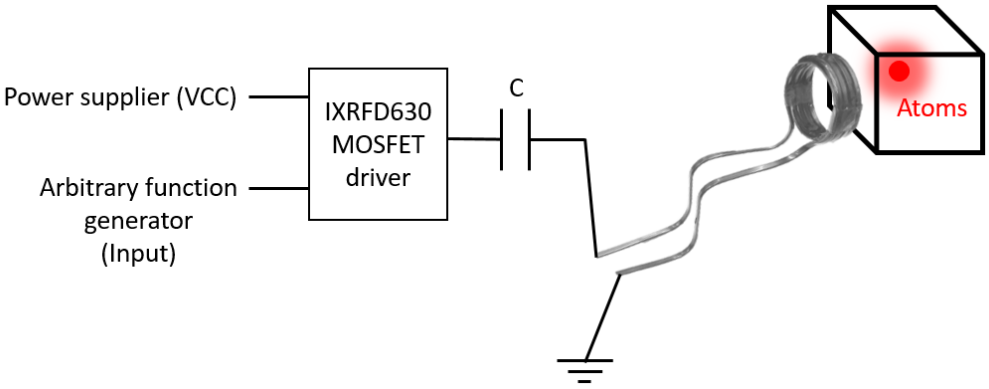

Fig. 6. Schematic description of the RF antenna circuit.

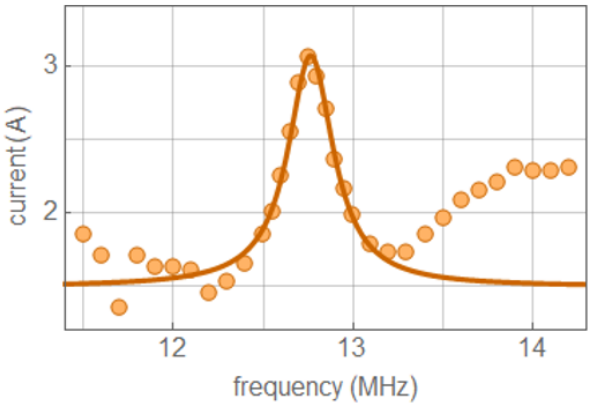

Fig. 7. Resonant behavior of the LC circuit. A Lorentzian fit (solid line) is made to the entire data set and in agreement with the measurements within about 1MHz around the resonance. The other data points probably indicate of current that is filtered out from the LC circuit.

In order to characterize the behavior of the circuit, we measured the current drawn by it from the power supplier for different input frequencies [See Fig. 7]. This data is

for a different antenna than the one we used in the experiment, but it demonstrate the behavior of the circuit very well for this section. A clear resonant behavior can be seen around 12.75 MHz. We obtain a 3A peak to peak current at resonance and a quality factor of $Q = \frac{f_0}{\Delta f} \cong \frac{12.5}{0.25} = 40$ which is considered to be relatively high for an RLC circuit at RF frequencies. We can also approximate L by a simple coil's inductance formula and extract C from $f_0 = \frac{1}{2\pi\sqrt{LC}}$. And since Q is also equal to $\frac{1}{R}\sqrt{\frac{L}{C}}$ we can see that $R \cong 5\Omega$ which is in agreement with the maximal current we obtain for a voltage of 15V.

Once it has been established that this circuit is indeed able to apply high amplitude magnetic field modulation at RF frequencies, we went a step further and duplicated it in order to have higher guaranty that the required shift of the molecular level is obtained. The second antenna is placed on the opposite side of the vacuum chamber, in a Helmholtz configuration. Since we cannot measure the magnetic field with an external sensor at the position of the atoms (inside the vacuum chamber), we tested the addition of the second antenna in a few different methods.

The first was to measure the modulation amplitude above the chamber. By using a field lines diagram, one could easily be convinced that the total amplitude above the chamber should be reduced once the Helmholtz configuration is applied. This is counter intuitive since the total amplitude at the location of the atoms is increased. We used a simple pickup antenna connected to a scope, so once alternating current runs through the antennas, induced field is created in the pickup antenna and we can observe a modulation on the scope with the same frequency and with an amplitude proportional to the amplitude of the original pulse. Table 1 shows the amplitude voltage on the pickup antenna for both connection configurations, Helmholtz and anti-Helmholtz. For each configuration the amplitude was measured when only the first antenna was operating, same with the

second antenna, and finally when both antennas were operating. It can be seen that for the Helmholtz configuration (as classified in retrospective) the amplitude is decreased when both antennas are operating, where for anti-Helmholtz the amplitudes are added up. This was the first validation that the second antenna does improve the signal. The second, more important validation will be laid out in section 4.2.4 after we describe a few other experimental procedures.

Table 1: Pick-up antenna amplitude - above the chamber.

	Antenna 1	**Antenna 2**	**Both antennas**
Anti-Helmholtz	12.5 V	8.8 V	20.7 V
Helmholtz	10 V	8 V	7.1 V

3.2 Experimental procedures

3.2.1 Number of atoms measurement

In each experimental sequence, we first load the atoms into the crossed dipole trap, after which the evaporation step is performed. During the evaporation, the bias magnetic field is turned on, and with several steps raised to its final value in which weakly bound Feshbach molecular state exists. Next, once desired temperature and density are achieved, the RF pulse is applied onto the atoms, by which molecules are formed. After the pulse is turned off we measure the number of free atoms left in the trap by absorption imaging.

A plain wave resonant with the free atoms is projected onto the atoms. The cloud shape in the plain perpendicular to the imaging laser propagation direction is a two

dimensional Gaussian. Therefore, in order to extract the number of atoms we use a single axis Gaussian fit, performed after an integration of the image with respect to the other axis. This measurement gives us the number of atoms in the trap up to a constant factor. The exact number of atoms is not relevant since we are only interested in the oscillatory behavior of the number of atoms as a function of pulse duration. The imaging is sensitive only to the atoms since the molecules are detuned 4MHz $\left(\frac{0.68}{\Gamma}\right)$ away from the resonance and the bandwidth of the laser is lower than the energy separation of the bound level from the free atoms. In addition, a waiting time is introduced to allow all molecules to decay from the trap.

For this experiment, the measurable quantity we desire is the MCE. For extracting that, we calculate $MCE(\tau) = \frac{N_0 - N(\tau)}{N_0}$, where N is the number of atoms in the trap, and τ is the pulse duration. This formula is the number of molecules produced divided by the initial number of atoms in the trap prior to applying the pulse.

3.2.2 Temperature measurement

A key parameter in this phenomena is the ensemble's temperature. It determines the typical time scale which sets the condition for non-adiabaticity. It also directly relates to the oscillations' frequency and contrast as described in the theoretical background. We therefore would like to independently measure the temperature since it would provide additional confirmation for the validity of the theory.

In our ultra-cold atoms system, we capture an atomic cloud in such densities that essentially it behaves like an ideal gas with a Maxwell Boltzmann temperature distribution. The atoms are distributed in a 3 dimensional Gaussian shape which is elongated along one axis (the optical trap laser propagation axis). Once the evaporation sequence is

complete, the trap is turned off, after which we wait for a certain amount of time before taking an absorption image to extract the atoms' distribution. It is easy to show that with an initial Gaussian spatial distribution, the expansion of the thermal cloud remains Gaussian, with a width that grows with time as $\sigma_t^2 = \sigma_0^2 + \frac{Tk_B}{m}t^2$, when σ^2 is the Gaussian variance, T is the temperature, and k_B is the Boltzmann constant.

In order to extract the temperature of the system, a series of measurements, in which the time between the turn-off of the trap and the imaging time, i.e the time of flight (TOF), is varied. By ploting σ_t^2 as a function of t^2 and applying a linear fit, the temperature can be extracted from the slope. An example of such sequence is presented in Fig. 8 with the typical temperature we achieve in our system, i.e $T \approx 2\mu K$.

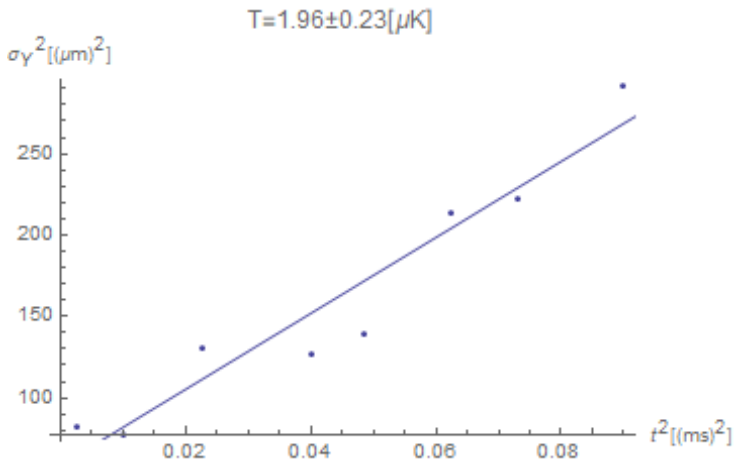

Fig. 8. An example of a temperature measurement. The line is a linear fit for σ^2 as a function of the time of flight squared.

3.2.3 Resonance field calibration

The Feshbach molecule binding energy is well known for different scattering lengths [18, 19]. In our system we apply our DC magnetic field by running high currents in 2 coils

surrounding the trap, but we can only know the magnetic field the atoms feel up to some precision. In order to more accurately determine the field strength, we perform a resonance measurement. As described in the theoretical background, the Feshbach binding energy depends on the scattering length which can be tuned by the magnetic field. In this experiment we get the atoms to their final temperature and then set the magnetic field to some value. Next we apply an RF pulse of $\sim 1ms$ at a frequency which corresponds to the binding energy at the set field. We repeat this procedure while changing the bias magnetic field at the time of the pulse from one run to another. When the binding energy E_b defined by the magnetic field matches the pulse frequency, the efficiency of molecule production is optimized. However, there are two important broadnings to this calibration method. The first, as mentioned earlier, is the thermal distribution of the free atoms from which the molecule is formed. The second is the fact that the current that creates the bias magnetic field in our lab is stabilized to a precision of $\sim 5 \cdot 10^{-5}$ (STD). Therefore, the line we're expecting is a convolution of a Maxwell-Boltzmann distribution at temperature T, with a Gaussian distribution with $\sigma \approx 50mG$. In most measurements we make, with a temperature $T \approx 1.5\mu K$, the MB distribution has a width of $\frac{k_B T}{h} \approx 30kHz$. The magnetic field instability in this case swallow the thermal distribution, so it can be taken as a delta function without any noticeable difference from the precise function. So we can determine the exact magnetic field by applying a Gaussian fit to the data and extracting the center. Fig. 9 shows an example of such an experiment. A clear resonance can be seen at $\sim 874.77G$ with a contrast of $\sim 35\%$.

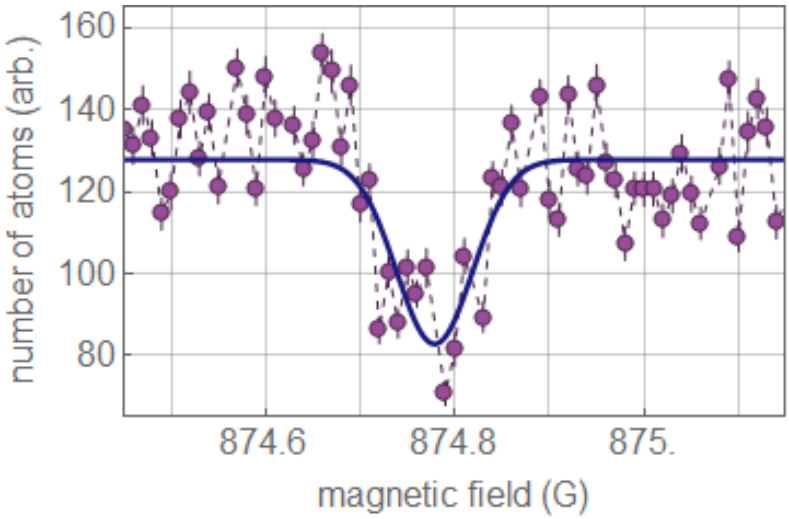

Fig. 9. Number of free atoms left in the trap after applying a 1ms pulse at a frequency of 12.8MHz as a function of the DC magnetic field. The solid line is a Gaussian fit to the data.

3.2.4 Shift in resonance due to field modulation

In order to observe interference we need to be able to shift the bound energy level by more than the temperature, which is $\sim 1\mu K$. The pulse intensity is determined by the magnetic field modulation amplitude b, so the magnetic field the atoms experience is $B(t) = B_0 + b\,sin(\omega t)$. As mentioned before, the binding energy depends on the scattering length as $E_b = -\frac{\hbar^2}{ma^2}$ and in turn, the scattering length depends on the external magnetic field as $a(B) = a_{bg}(1 - \frac{\Delta}{B-B_0})$, therefore by applying the pulse we simultaneously also modulate the required frequency for transition. With a simple derivation, it is possible to show that the effective resonance field is shifted due to this modulation.

First, we will write the scattering length during the pulse:

$$a(B) = a_{bg}(1 - \frac{\Delta}{(B-B_0)+b\,sin(\omega t)})$$

In our experiment the following is usually satisfied $b \ll (B - B_0) \ll \Delta$, so we can simplify

the expression around $b = 0$ to be

$$a(B) = -\frac{a_{bg}\Delta}{B-B_0}\left[1 - \frac{b}{B-B_0}sin(\omega t)\right] = a_c\left[1 - \frac{b}{B_c-B_0}sin(\omega t)\right]$$

where $a_c \equiv -\frac{a_{bg}\Delta}{B_c-B_0}$ is the scattering length for vanishing modulation amplitude, and $E_b(B_c)$ is the binding energy that's corresponds to the pulse frequency, i.e $E_b = \hbar\omega$, for $b = 0$. Substituting this in the energy gives us

$$E(t) = -\frac{\hbar^2}{ma_c^2}\frac{1}{\left[1-\frac{b}{B_c-B_0}sin(\omega t)\right]^2}$$

If we expand this expression for $\frac{b}{B_c-B_0} \ll 1$ we get

$$E(t) = -\frac{\hbar^2}{ma_c^2}\left[1 + 2\frac{b}{B_c-B_0}sin(\omega t) + 3\left(\frac{b}{B_c-B_0}\right)^2 sin^2(\omega t)\right]$$

And finally, averaging over time result in

$$\langle E(t)\rangle \approx -\frac{\hbar^2}{ma_c^2}\left[1 + \frac{3}{2}\left(\frac{b}{B_c-B_0}\right)^2\right]$$

So we can see that the binding energy addressed during the pulse, will effectively shift towards higher values and depends quadratically in the modulation amplitude. However, it is important to remember that when calibrating the magnetic field, we do not scan the frequency, but the DC magnetic field. The pulse frequency $f = \frac{\omega}{2\pi}$ remain constant in our system and therefore, the optimal point in which we produce the maximal number of molecules is when the binding energy corresponds to that frequency, i.e when $\langle E(t)\rangle = \hbar\omega$. And so the DC magnetic field in which we will find the resonance will shift as well. We can substitute that constraint in the equation and extract the detected resonance field B_c^{det} from it:

$$\hbar\omega = \frac{\hbar^2}{m}\frac{(B_c^{det}-B_0)^2}{(a_{bg}\Delta)^2}\left[1 + \frac{3}{2}\left(\frac{b}{B_c^{det}-B_0}\right)^2\right]$$

We keep in mind that we work in the area of $B < B_0$ where there is a weakly bound Feshbach molecule, so after some algebra we get

$$B_c^{detect} = B_0 - \Delta_B \sqrt{1 - \frac{3}{2}\left(\frac{b}{\Delta_B}\right)^2}$$

where $\Delta_B^2 = \frac{\omega m \left(a_{bg}\Delta\right)^2}{\hbar}$ is the distance of the resonance field from the Feshbach resonance for vanishing modulation. In our system $\Delta_B \approx 10G$ and the modulation amplitude $b \approx 2G$ so $\left(\frac{b}{\Delta_B}\right)^2$ can be treated as a small parameter and it is possible to expand the expression up to second order

$$B_c^{detect} = B_0 - \Delta_B \left[1 - \frac{3}{4}\left(\frac{b}{\Delta_B}\right)^2\right] = B_c^{bare} + \frac{3}{4}\frac{b^2}{\Delta_B}$$

So we see that in the range of parameters used in our lab, there is a quadratic shift in the resonance field detected, as we increase the modulation amplitude.

Since we cannot directly measure the magnetic field modulation amplitude at the atoms' location, we must use alternative approaches. Our best indication of the amplitude is through the current the VCC supplier supplies. As described in section 4.1.2, the drive from the supplier is on during half duty cycle, so the current shown on its display is half of the current amplitude in the circuit. For each voltage combination, we turned the pulse on and wrote down the current on each supplier. We considered the atoms to be in the center of a symmetric Helmholtz configuration, so the contribution to the field per Amper of each coil is the same, allowing us to add up these numbers to a total current, and the latter is the parameter shown on the horizontal axis of the graph.

Fig. 10 shows the resonance field measured for different modulation amplitudes. These measurements were taken in 3 different days, each day with at least 4 points. The magnetic field in our lab is stabilized along the duration of a specific day, but it can have systematic shift between different days due to the turn off and on of the power suppliers. In order

to compensate for this shift, we performed a quadratic fit for the data of each day and subtracted the bias field for zero modulation amplitude, as determined by the fit. The results were then combined into one data set after which the final fit was performed.

From the fit, together with the theory shown earlier in this section, we could extract the conversion parameter between the current provided by the suppliers to the field generated in the atoms' location. according to a relation of $b = \alpha I_{total}$ We got $\alpha = 0.55\frac{G}{A}$. From a geometric point of view, calculating the same coefficient for the 2 coils we use to generate the pulse, we get $\alpha = 0.73\frac{G}{A}$. Therefor, it seems that $\sim 25\%$ of the current does not flow through the antennas, which is within reasonable behavior.

We can also see that we achieve a total shift of $> 180mG$ in the resonance magnetic field, which is, in our area of interest, equivalent to $\sim 100KHz$. The shift is more than 3 times our temperature, meaning that we can reach the amplitudes required for observing oscillations.

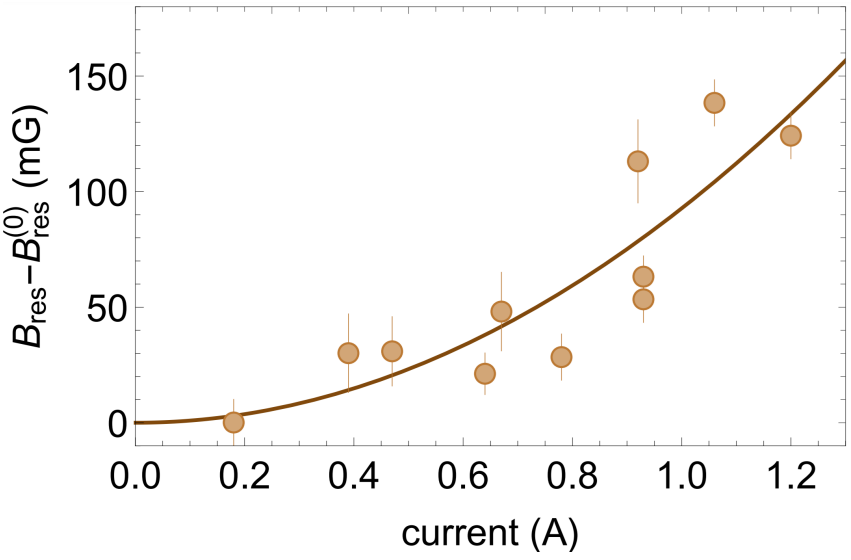

Fig. 10. Resonance DC magnetic field B_0 as a function of the modulation amplitude b as measured at pulse frequency $f = 4.02MHz$. The solid line is a quadratic fit of the data.

3.2.5 Pulse rise time

Another key feature of Stückelberg oscillations is non-adiabaticity. The coupling Hamiltonian is governed by the RF pulse, therefor its turn on and off time scale is the parameter that determines the existence of adiabaticity in the system. This time scale is compared to the time scale of the bare hamiltonian, which is determined by the energy width of the thermal gas, i.e $\tau_{bare} = \frac{h}{k_B T}$. For $T = 1.5\mu K$ we get $\tau_{bare} \approx 32\mu s$.

We wanted to confirm we meet the condition for non-adiabaticity, so we measured the pulse shape to extract from it the rise and fall time. We did that by placing a pickup antenna near one of the antennas and recording the induced signal in it. This was sufficient since for this purpose we are not interested in the amplitude of the signal, but only the time behavior of it. We've come to learn that producing the RF pulse, carries with it some minor noise at other frequencies, mostly higher harmonics of the carrier frequency. These frequencies have negligible coupling so we filtered them out in order to extract the time scale of the pulse. Fig. 11 shows the pulse's envelope with an exponential fit (according to the easily derived and known thoery of an RLC circuit). The time scales for the turn on (off) of the pulse is $4.42\mu s$ ($4.53\mu s$), so we can see that this is an order of magnitude shorter than the time scale of the system τ_{bare}, therefor non-adiabaticity is satisfied.

3.3 Results

3.3.1 Observation of oscillations

In section 4.1 and 4.2 we have shown that indeed we meet the conditions for observing oscillations. Therefore the next step was to go ahead and measure them. To give ourselves the best chances for success, we used parameters in the edge of our reach that bring out

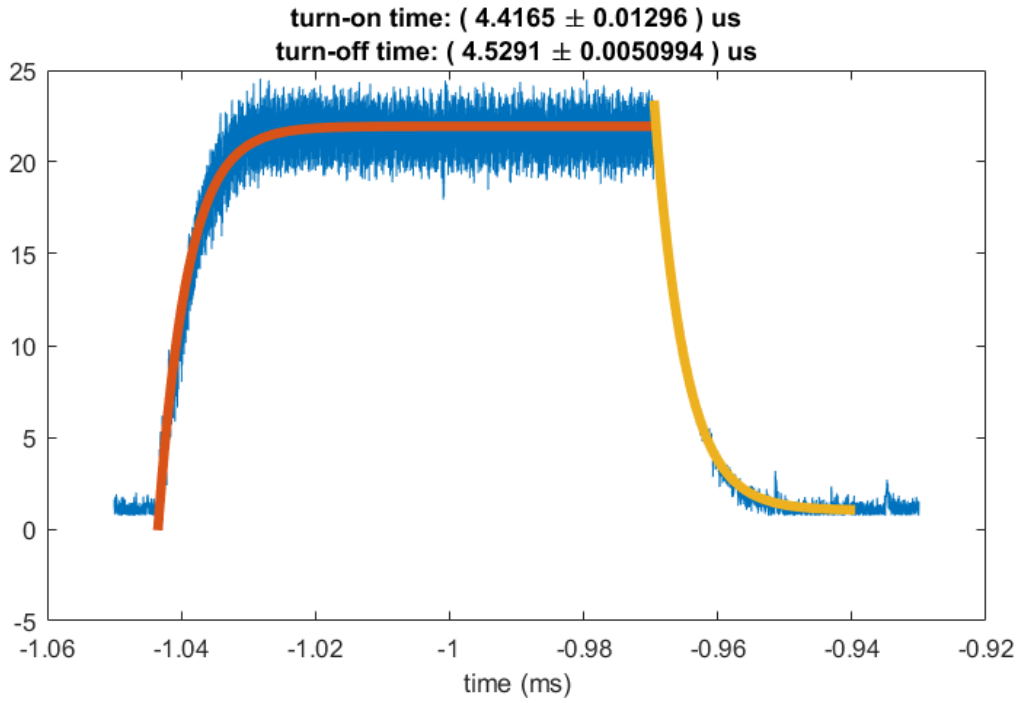

Fig. 11. Pulse amplitude (envelope) after moving-average smoothing. Orange (yellow) line is the analytical solutions for the turn on (off) of a resonantly driven RLC circuit. Exponent time scales are extracted from the fit and presented above.

the largest contrast and highest frequency. As seen in section 3.5, this means that we aimed for the lowest temperature and largest modulation amplitude we could achieve.

The bias magnetic field in the lab is stabilized at $\sim 884G \pm 40mG$, but it may fluctuate from one day to another, due to the turn off and on of the power supplier. Therefore we must calibrate the bias magnetic field in the beginning of each day. However, there is importance to the modulation amplitude used for this calibration since it can shift the resonance. In order to get the desired effect, in which the maximal shift is obtained with optimal molecule production in the beginning and end of the pulse, the resonance is calibrated for low modulation amplitude (optimally for zero amplitude), which in our case is 3V VCC for each RF generator circuit. Lower voltage is not possible due to operation

limitations posed by the MOSFET driver. However, Fig. 10 shows that the resonance for zero voltage is only a few mG away from the resonance for 3V, which is an order of magnitude lower than the bias field stability, and therefor irrelevant.

In each run, $\sim$ 25000 atoms were loaded into a trap, and the bias magnetic field is set to the low field resonance. Once this is done, an RF pulse at $4.02MHz$ is applied onto the atoms. In order to get the maximal shift, the voltage for each circuit is set to be 10V. The oscillations are of the MCE as a function of the pulse duration, and so this is the parameter that is varied from one run to another. The resolution of this parameter is of $2\mu s$. Whenever the pulse duration does not divide with this quantity, it is rounded downwards by the control system. After the pulse ends, the number of free atoms left in the trap is measured as described in section 4.2.1. The molecules produced in this sequence are still in the trap at the time of measurement, however due to the large energy separation, we are blind to them and they do not absorb the imaging laser. We measured this for pulses duration of 2 to 82 μs with an averaging of 8 runs per data point. The results are shown in Fig. 12.

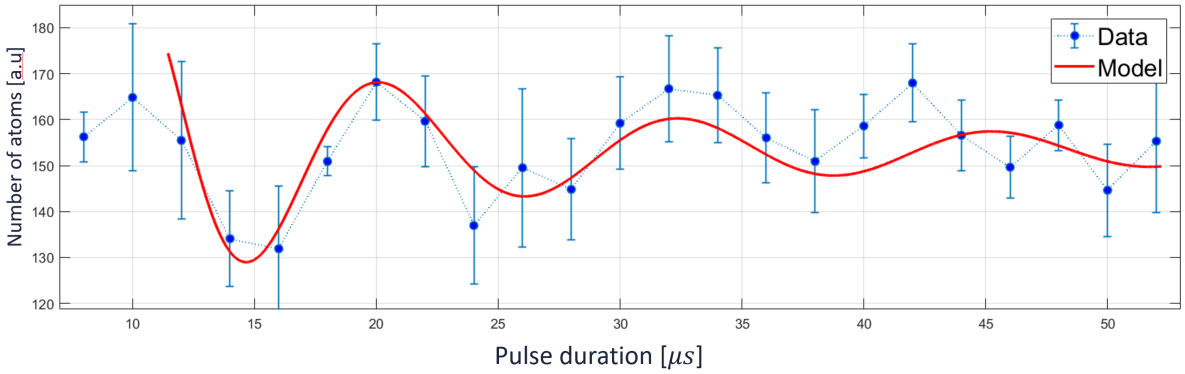

Fig. 12. Experimental data (blue) at the best conditions for observing oscillations. An approximated model from [2] was drawn together with the data (red) with parameters chosen visually in a tailor made program.

It is possible to see a deep minimum in the number of atoms right in the beginning of the graph. This minimum corresponds to the first maximum in (figure of theory) which describes the behavior of the MCE. It is also clear to see that there is a revival in the number of atoms later on in the graph. This is an important feature that sets the difference from any other incoherent molecule production procedure.

3.3.2 Monotonic decay

In order to further convince ourselves in the validity of this result, we decided to examine a different scenario. We kept the modulation amplitude and frequency the same, while ramping up the bias magnetic field to its high-amplitude resonance value. The result can be seen in Fig. 13, which shows a monotonic decrease in the number of free atoms left in the trap, this of course means a monotonic increase in the MCE.

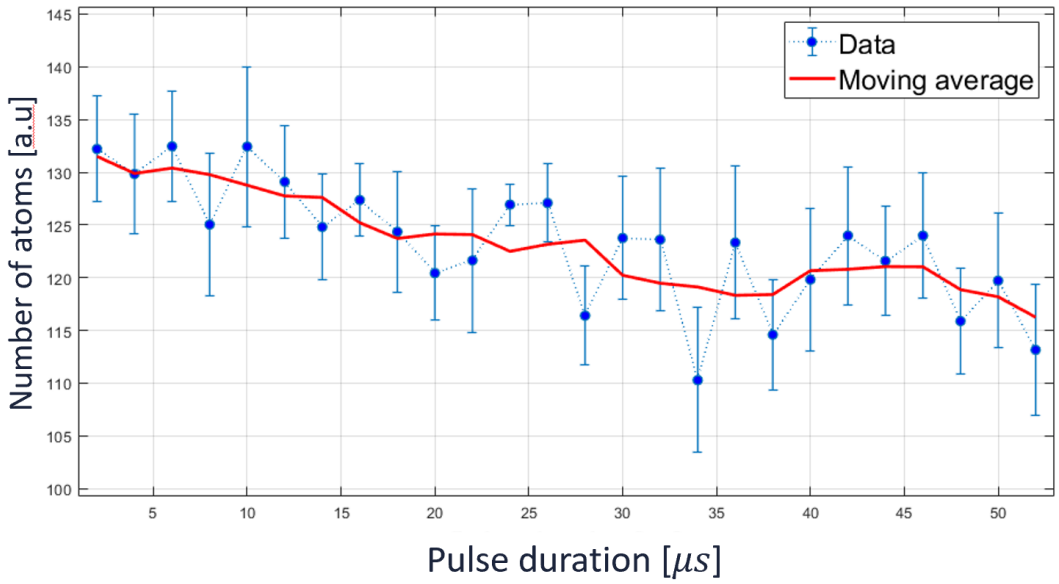

Fig. 13. Number of atoms left at the end of the trap as a function of pulse duration for bias magnetic field set as the high amplitude resonance. A monotonic decay in the number of atoms can is obsereved.

This can be understood by the same model used for explaining the oscillations and is described in Fig. 14. By ramping up the DC magnetic field, we decrease the binding energy, setting the bound level energy to a higher value (due to its negative sign). Since the pulse frequency remains the same, in the beginning of the pulse, there is no coupling between the free atoms and the bound level. As the pulse envelope rises, the shift takes the bound level into the major part of the continuum and the coupling appears. Since we took the bias field to be the resonant field for high amplitude, the result is that during the majority of the pulse, the bound level is coupled to the continuum and molecules are being produced. Therefore there is no interferometer and the longer the pulse lasts, the more molecules are being produced. The results shown here do carry some noise, but the main difference from the results in section 4.3.1 is that here it is clear that there is no revival in the number of atoms lefts in the trap at the end of the sequence, Only a monotonic decay.

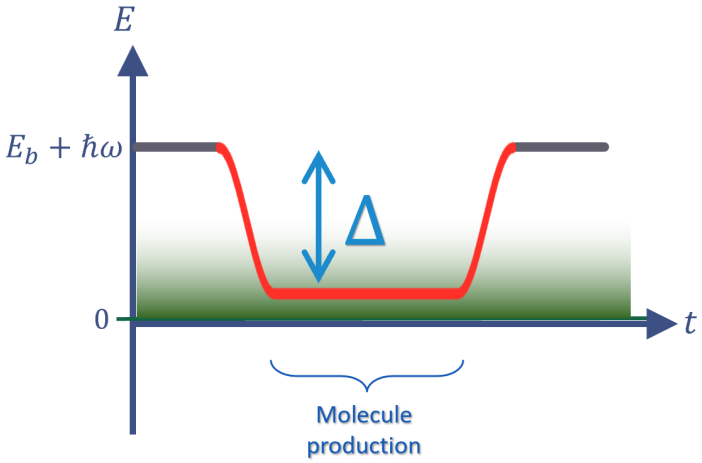

Fig. 14. Energy diagram for the high bias field scenerio. The molecular state at the beginning and end of the pulse is decoupled from most of the continuum. As the pulse amplitude approach its maximum value, the coupling occur and molecules are produced. As the pulse duration is extended, more molecules are produced, but in a non coherent manner since the molecular level is embedded within the continuum.

3.4 Experiment - Theory comparison

The graphs in Ref. [2] are made for a different system of ^{85}Rb atoms, so we could not compare our results directly with their model. Even if their model was done on ^{7}Li, still we would have to operate with the parameters similar enough to the ones used in the theory. We do conduct a collaboration with the same theoretical team these days for an upcoming paper, but for this thesis we will show a more "within reach" approach that allows us to evaluate the agreement of the experiment with the proposed theory.

The model we used is equation 6 in Ref. [2], which is an approximated solution of the MCE as a function of the pulse duration. We did not use explicitly all the parameters in that solution, rather simplified them further to a few general parameters, some with a somewhat intuitive meaning. However, our main interest is that the behavior of the function fits our data.

Fig. 12 shows that data of section 4.3.1 together with the model function for parameters we set manually. The parameters were set to these values after varying them by hand in a tailored program within a large range, visually determining a combination that fits best to our data. Two parameters are very much worth mentioning. One is the temperature, which for this model line was found best to fit at $T = 1.5\mu K$. It is important to mention here that since this is not a formal fitting procedure, we could have probably go to temperatures within $\pm 0.2\mu K$ from that value, but any further than that and the model did not fit the data any more. The number 1.5 was conveniently chosen since we know that this is the temperature in our system, but the remarkable this here that this is also more or less that parameter that fits best to our data.

Same can be said about the maximal shift of the molecular level during the pulse. The parameter used for the model line was $\Delta = 107\, kHz$ which is very close to the actual

value measured independently, as described in section 4.2.4 to be $112\,kHz$.

We can see amazing agreement between the experimental data and the theory. This might be the strongest evidence for the validity of this model, and despite being only an approximated solution of the MCE, it allows great optimism for further research and accurately comparing the theory with the experiment.

4 Conclusions and outlook

We have successfully managed to produce a system that can put to test the theory suggested in [2]. Within our results, we see evidence of coherency, that according to a few theoretical analyzes is far from trivial. Moreover, the remarkable correspondence between the obtain data of oscillations and the model increases our understanding of similar quantum systems, specifically to the field of cold atoms and molecules.

Having said that, the results shown in this thesis are still merely the opening shot to a wide range of research possibilities. This phenomenon contains many parameters, e.g temperature, binding energy, pulse amplitude and frequency, and many more. These parameters and their influence can be explored and bring greater knowledge of the behavior of systems that contain a combination of discrete and continuous states.

Also, these days we are collaborating with a group of theoreticians in order to find more rigorous agreement between theory and experiment. Even though the outlines of both systems is rather similar, still there are many differences that must be reconcile in order to complete our understanding of the process at hand. These include the pulse form, different energy and temperature scale, and more. We see great promise in this process and expect to publish in the very near future.

Finally, this work brings additional clarity to the process of molecule formation, which had some vagueness around the ability to achieve coherence. It shows that by following a different protocol, Stückelberg oscillations can be seen, in the same system where the Rabi sequence fails. We believe this would open the path for much research to come in the field of atomic and molecular physics.

References

[1]Q. Ning, U. Saalmann, and J. Rost, "Electron dynamics driven by light-pulse derivatives", Phys. Rev. Lett. **120**, 033203 (2018).

[2]P. Giannakeas, L. Khaykovich, J. Rost, and C. Greene, "Nonadiabatic molecular association in thermal gases driven by radio-frequency pulses", Phys. Rev. Lett. **123**, 043204 (2019).

[3]S. Thompson, E. Hodby, and C. Wieman, "Ultracold molecule production via a resonant oscillating magnetic field", Phys. Rev. Lett. **95**, 190404 (2005).

[4]Y. Ding, J. Pérez-Ríos, and C. Greene, "Effective atom–molecule conversions using radio frequency fields", Chem. Phys. Chem. **17**, 3756–3763 (2016).

[5]O. Machtey, Z. Shotan, N. Gross, and L. Khaykovich, "Association of efimov trimers from a three-atom continuum", Phys. Rev. Lett. **108**, 210406 (2012).

[6]T. Tscherbul and S. Rittenhouse, "Three-body radio-frequency association of efimov trimers", Phys. Rev. A **84**, 062706 (2011).

[7]Y. Ding, J. D'Incao, and C. Greene, "Effective control of cold collisions with radio-frequency fields", Phys. Rev. A **95**, 022709 (2017).

[8]P. Demekhin and L. Cederbaum, "Dynamic interference of photoelectrons produced by high-frequency laser pulses", Phys. Rev. Lett. **108**, 253001 (2012).

[9]M. Saffman, "Quantum computing with atomic qubits and rydberg interactions: progress and challenges", Journal of Physics B: Atomic, Molecular and Optical Physics **49**, 202001 (2016).

[10]M. Saffman, T. G. Walker, and K. Mølmer, "Quantum information with rydberg atoms", Rev. Mod. Phys. **82**, 2313–2363 (2010).

[11]M. Ivanov, R. Kienberger, A. Scrinzi, and D. Villeneuve, "Attosecond physics", Journal of Physics B: Atomic, Molecular and Optical Physics **39**, R1–R37 (2005).

[12]C. Cohen-Tannoudji and D. Guéry-Odelin, *Advances in atomic physics* (WORLD SCIENTIFIC, 2011).

[13]C. Chin, R. Grimm, P. Julienne, and E. Tiesinga, "Feshbach resonances in ultracold gases", Rev. Mod. Phys. **82**, 1225–1286 (2010).

[14]T. Hanna, T. Köhler, and K. Burnett, "Association of molecules using a resonantly modulated magnetic field", Phys. Rev. A **75**, 013606 (2007).

[15]N. Ramsey, "A molecular beam resonance method with separated oscillating fields", Phys. Rev. **78**, 695–699 (1950).

[16]E. Hodby, S. T. Thompson, C. A. Regal, M. Greiner, A. C. Wilson, D. S. Jin, E. A. Cornell, and C. E. Wieman, "Production efficiency of ultracold feshbach molecules in bosonic and fermionic systems", Phys. Rev. Lett. **94**, 120402 (2005).

[17]N. Gross, *Experimental study of universal three-body physics with ultracold bosonic lithium* (Bar Ilan University, 2011).

[18]P. Julienne and J. Hutson, "Contrasting the wide feshbach resonances in li 6 and li 7", Phys. Rev. A **89**, 10.1103/PhysRevA.89.052715 (2014).

[19]N. Gross, Z. Shotan, O. Machtey, S. Kokkelmans, and L. Khaykovich, "Study of efimov physics in two nuclear-spin sublevels of 7li", English, Comptes Rendus Physique **12**, 4–12 (2011).

תקציר

כאשר מפעילים צימוד רזונטיבי על מערכת 2 רמות קוונטית, מתקבלות אוסילציות באכלוס של כל רמה כפונקציה של משך זמן הצימוד. תופעה זו נקראת בשם "אוסילציות רבי", וכיום הינה ידע בסיסי במכניקה קוונטית. מאז גילויה של התופעה, הייתה התקדמות רבה במחקר בכיוון זה. החל מרצף "רמזי", אשר מנצל את השליטה העדינה של פולס "רבי" על אוכלוסיית כל רמה, ועד לתהליכים מורכבים יותר, המתוארים לעיתים קרובות באלגנטיות על ידי ספירת בלוך.

על ידי החלפת אחת הרמות הבדידות בספקטרום אנרגטי רציף, המערכת המתקבלת הינה מסובכת יותר, וכמעט בלתי אפשרי למדוד אוסילציות "רבי" תחת תנאים מסויימים. מערכת שכזו יכולה להמצא בתהליכי יינון, בהם אלקטרון קשור מצומד למצבי רצף של אלקטרון חופשי. תרחיש נוסף, רלוונטי יותר לסיפור שלנו, הוא המקרה של ייצור מולקולות מאטומים בודדים חופשיים. המקרה השני מכיל תת-תחום רחב ומתפתח בשם מולקולות פשבך.

בזכות הטמפרטורות העל-נמוכות המושגות כיום במערכות אטומים קרים, אפשרי לנצל בקלות יחסית את היתרונות שמציעה תיאורית פשבך של תהודות בתהליכי התנגשות בין חלקיקים. התיאוריה חוזה את ההמצאות של תהודות בין מצבי ספין שונים אשר מאפשרים יצירה של מולקולות "חלשות" מאטומים חופשיים. החלק החדשני בתופעה זו הוא שניתן לכוון את אנרגיית הקשירה בין האטומים על ידי שדה מגנטי חיצוני.

בעבודה זו, אנו נתאר מערכת בה מופעל צימוד אוסילטורי רזונטיבי בין רמה בדידה ורצף אנרגטי, ונראה כיצד אוסילציות באוכלוסיה מופיעות. אולם אוסילציות אלו שונות בטבען מאוסילציות רבי המפורסמות. התופעה הזו נקראת אוסילציות שטוקלברג, וזהו אפקט לא אדיאבטי, הקשור למעטפת הפולס, אשר נצפתה עד כה רק בתהליכי יינון על ידי פולסים אולטרה קצרים [1]. התיאוריה לתהליך זה הוצגה במאמר [2], ואנו שמנו לעצמנו למטרה למדוד ולצפות בתופעה הנ"ל במערכת של אטומים אולטרה קרים. התוצאות הנסיוניות שופכות אור על ההתנהגות של מערכות תחת צימוד אוסילטורי, והן קריטיות להבנה של תהליכים דומים רבים.

עבודה זו נעשתה בהדרכתו של פרופ' לב חייקוביץ' מהמחלקה לפיזיקה,
אוניברסיטת בר אילן.

אוניברסיטת בר-אילן

מדידה של אוסילציות קוהרנטיות בייצור מולקולות מגז תרמי אולטרה-קר

רועי אלבז

עבודה זו מוגשת כחלק מהדרישות לשם קבלת תואר מוסמך במחלקה לפיזיקה,

באוניברסיטת בר אילן

רמת גן, ישראל ה'תשפ"ב